Applied Physics Letters

Optical absorption edge broadening in thick InGaN layers: Random alloy atomic disorder and growth mode induced fluctuations

Cite as: Appl. Phys. Lett. **112**, 032106 (2018); https://doi.org/10.1063/1.5010879
Submitted: 27 October 2017 . Accepted: 28 December 2017 . Published Online: 17 January 2018

Raphaël Butté, Lise Lahourcade, Tomas Kristijonas Uždavinys, Gordon Callsen, Mounir Mensi, Marlene Glauser, Georg Rossbach, Denis Martin, Jean-François Carlin, Saulius Marcinkevičius, and Nicolas Grandjean

AIP Publishing

Optical absorption edge broadening in thick InGaN layers: Random alloy atomic disorder and growth mode induced fluctuations

Raphaël Butté,[1,a)] Lise Lahourcade,[1,b)] Tomas Kristijonas Uždavinys,[2] Gordon Callsen,[1] Mounir Mensi,[2] Marlene Glauser,[1] Georg Rossbach,[1,b)] Denis Martin,[1] Jean-François Carlin,[1] Saulius Marcinkevičius,[2] and Nicolas Grandjean[1]
[1]*École Polytechnique Fédérale de Lausanne (EPFL), Institute of Physics, CH-1015 Lausanne, Switzerland*
[2]*Department of Applied Physics, KTH Royal Institute Technology, Electrum 229, S-16440 Kista, Sweden*

(Received 27 October 2017; accepted 28 December 2017; published online 17 January 2018)

To assess the impact of random alloying on the optical properties of the InGaN alloy, high-quality $In_xGa_{1-x}N$ ($0 < x < 0.18$) epilayers grown on *c*-plane free-standing GaN substrates are characterized both structurally and optically. The thickness (25–100 nm) was adjusted to keep these layers pseudomorphically strained over the whole range of explored indium content as checked by x-ray diffraction measurements. The evolution of the low temperature optical absorption (OA) edge linewidth as a function of absorption energy, and hence the indium content, is analyzed in the framework of the random alloy model. The latter shows that the OA edge linewidth should not markedly increase above an indium content of 4%, varying from 17 meV to 30 meV for 20% indium. The experimental data initially follow the same trend with, however, a deviation from this model for indium contents exceeding only ~2%. Complementary room temperature near-field photoluminescence measurements carried out using a scanning near-field optical microscope combined with simultaneous surface morphology mappings reveal spatial disorder due to growth meandering. We conclude that for thick high-quality pseudomorphic InGaN layers, a deviation from pure random alloying occurs due to the interplay between indium incorporation and longer range fluctuations induced by the InGaN step-meandering growth mode. https://doi.org/10.1063/1.5010879

Since the first report of high-brightness blue light-emitting diodes (LEDs),[1] III-nitride based light emitters have impacted many aspects of our life. This is illustrated through the revolution of solid-state lighting by high luminous efficacy white LEDs[2] and high-density data storage relying on blue-violet laser diodes (LDs).[3] In addition to efficient *p*-type doping, the key-enabling feature behind those technologies is the use of an InGaN-based active region characterized by a remarkable insensitivity against dislocations.[4] Early explanations relied on composition fluctuations originating from thermodynamic instability,[5] leading to indium-rich clusters preventing carriers from diffusing into non-radiative recombination centers.[6,7] Later, structural investigations using transmission electron microscopy (TEM) revealed that those clusters were induced by a long exposure to electron beam irradiation and hence are not genuinely present in the pristine InGaN alloy.[8] The most favored current explanation allowing us to account for the unusual emission properties of this alloy invokes the presence of In-N-In-N-In-zigzag chains.[9–11] Recently, a series of theoretical works focusing on disorder in semiconductors based on a so-called *localization landscape* picture provided new insights into the optical features of optoelectronic devices relying on an InGaN/GaN quantum well (QW) medium.[12–14] Nonetheless, because many of the previous optical studies were performed on QWs grown along the polar *c*-axis, the subsequent analyses of this ternary alloy were plagued by the complexity of such systems. Indeed, the understanding of their optical properties is made more intricate compared to bulk layers due to additional difficulties in disambiguating the exact contribution due to QW thickness fluctuations from compositional fluctuations in emission and/or absorption features. Furthermore, *c*-plane QW transition energies are known to be affected in an opposite manner by carrier confinement and the built-in electric field.[15] Even for nonpolar InGaN/GaN QW heterostructures where the critical role played by carrier localization in the Auger recombination process has been unambiguously evidenced,[16] the microscopic picture of such a ternary alloy remains an intricate one. Therefore, studies carried out on thick InGaN epilayers are especially relevant as they allow minimizing the number of degrees of freedom.[17–24] However, the vast majority of the previous investigations was performed on InGaN epilayers grown on sapphire for which the threading dislocation density remains significant ($>10^8\,cm^{-2}$). The latter can induce local strain field variations and spiral growth that may locally change the incorporation of indium atoms. In this respect, investigating the optical properties of high-quality InGaN epilayers grown on *c*-plane free-standing (FS) GaN substrates should prove complementary to recent structural information, namely, compositional mapping, obtained on InGaN QWs using TEM.[25,26] One important aspect deals with the further elucidation of the driving mechanisms behind alloy disorder, whose weight as a function of indium content can be probed via the combination of optical absorption (OA) and near-field

a)Author to whom correspondence should be addressed: raphael.butte@epfl.ch
b)Present address: OSRAM Opto Semiconductors GmbH, 93055 Regensburg, Germany.

optical measurements. In particular, one interesting outcome would consist in establishing a more comprehensive connection between the optical properties of those layers and the surface morphology induced by InGaN growth conditions, namely, step-meandering.[27]

In this work, we investigate the structural and optical properties of $In_xGa_{1-x}N$ ($x < 0.18$) epilayers grown on *c*-plane FS GaN substrate by metalorganic vapor phase epitaxy (MOVPE). Their thickness (25–100 nm) was chosen in order to prevent the occurrence of any unwanted compositional inhomogeneities driven by plastic relaxation. The evolution of the OA edge linewidth as a function of absorption energy and hence indium content is analyzed in the framework of the conventional random alloy model.[28] We found that the OA edge linewidth primarily originates from pure random atomic disorder until meandering growth induces large scale indium composition fluctuations.

InGaN epilayers were grown in an MOVPE reactor on low dislocation density ($\sim 1 \times 10^6\,cm^{-2}$) *c*-plane FS GaN substrates with a surface misorientation in the range of 0.3° to 0.5°. They were deposited at temperatures between ~700 and 850 °C using N_2 as carrier gas. These growth conditions are those used for the realization of LDs.[29] An overview of the characterization techniques can be found in Sec. A of the supplementary material. The indium content, which should nominally cover the ~0.4 to 18% range, was determined by high-resolution x-ray diffraction (HRXRD) measurements. A relative uncertainty better than ±7% deduced from symmetric $\omega - 2\theta$ x-ray diffraction (XRD) scans is achieved, which corresponds to an absolute uncertainty less than 1% for a targeted indium content of 10%. Those measurements were complemented by two-dimensional (2D) reciprocal space mappings (RSMs) to verify the strain state of the layers. RSM of the $\langle 10\bar{1}5 \rangle$ asymmetric reflections of the GaN and InGaN layers is shown for a medium indium content layer (8.6 ± 0.2%) in Fig. 1. It is clearly observed that this sample is pseudomorphic to GaN as the InGaN peak is symmetric and centered at the reciprocal lattice coordinates of the FS GaN substrate. In fact, we can rule out any plastic relaxation for our 100-nm-thick InGaN epilayers up to an indium composition of 8.6%, a result which is overall consistent with the expected critical thickness values.[30] Note that for the latter sample, the width of the 2θ reflection peak is larger than that of its lower indium-content counterparts, which could originate from more pronounced long-range In fluctuations. Fits to the corresponding $\omega - 2\theta$ XRD scan are compatible with an indium content ranging from 8.4 to 8.8%. In order to avoid issues related to the above-mentioned relaxation (see Table I), the thickness of InGaN epilayers with a targeted indium content larger than 9% was voluntarily limited to 25 nm. Such an approach allowed us to deal with pseudomorphic InGaN epilayers along the growth direction up to a value of ~18%. The reason behind the delayed plastic relaxation in the investigated InGaN epilayers, which is otherwise known to favor the incorporation of indium since it is driven by strain,[31] is twofold. Indeed, in contrast to previous reports in which InGaN epilayers were grown on *c*-plane sapphire substrates, the use of low dislocation density FS GaN substrates allows for an increase in the critical thickness before the onset of plastic relaxation as

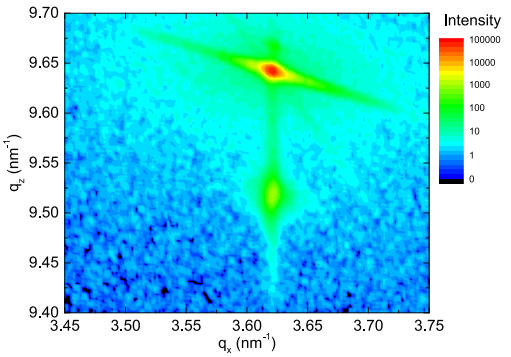

FIG. 1. XRD RSM of the $\langle 10\bar{1}5 \rangle$ asymmetric reflections of a 100-nm-thick InGaN epilayer with an indium content of 8.6%, which is pseudomorphic to GaN.

recently shown for GaN epilayers grown on AlN single crystals.[32] This effect is amplified by the need to decrease the growth temperature when targeting higher indium contents.

The evolution of the OA edge spectra extracted from low temperature (LT) ($T = 10$ K) micro-transmission measurements as a function of indium content is shown in Fig. 2. In addition to the expected energy redshift of the OA edge, a clear broadening of the excitonic features can be monitored with first a merger of the X_A and X_B transitions followed by their progressive disappearance in the band-to-band (BB) continuum due to the concomitant increase in the OA linewidth. Each OA spectrum is complemented by its corresponding LT photoluminescence (PL) spectrum measured at the same location on the sample. It is clearly seen that the LT PL linewidth and the related Stokes shift do not exhibit a monotonic increase with increasing indium content. This behavior illustrates the misleading information that can be inferred from these two quantities as PL does not probe the entire density of states, especially at LT. Instead, we will first focus on the OA measurements in order to provide more decisive information about the intrinsic or the extrinsic nature of the OA broadening in thick InGaN epilayers.

In Fig. 3(a), we show the evolution of the LT ($T = 10$ K) OA edge linewidth (Γ, filled green dots) as a function of the OA excitonic energy of several InGaN epilayers. Γ values

TABLE I. Relaxation degree (R) of 100-nm-thick InGaN epilayers as a function of indium content (x) deduced from XRD 2D-RSMs. For layers with an indium content in the 13%–15% range, the error bars on the relaxation degree (ΔR_+ and ΔR_-, above and below the quoted R value, respectively) clearly illustrate the onset of plastic relaxation with a transition from InGaN epilayers being pseudomorphic to GaN to epilayers that are partially relaxed. The relaxation state of the listed InGaN epilayers is indicated in the last column.

x	R	ΔR_+	ΔR_-	Relaxation state
0.026	0	0.04	0	Pseudomorphic
0.065	0	0.04	0	Pseudomorphic
0.070	0	0.04	0	Pseudomorphic
0.082	0	0.04	0	Pseudomorphic
0.086	0	0.04	0	Pseudomorphic
0.130	0	0.3	0	Onset of relaxation
0.146	0.15	0.05	0.14	Partially relaxed
0.175	0.06	0.06	0.04	Partially relaxed
0.185	0.08	0.06	0.04	Partially relaxed

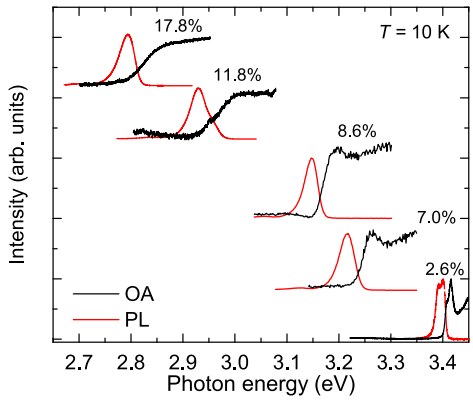

FIG. 2. OA edge spectra (black line) derived from LT micro-transmission measurements as a function of increasing indium content in pseudomorphic InGaN epilayers together with their corresponding PL spectrum. Each pair of spectra is vertically shifted for clarity.

were derived from a deconvolution of micro-transmission spectra considering the combination of two Gaussian excitonic lines and a sigmoid function of the same broadening, which is shifted to higher energies by the exciton binding energy for the BB continuum. The calculated dependence of the expected linewidth for a random alloy[28] is also reported for the fully strained case (orange line, see supplementary material, Secs. C and D for details). For an indium content lower than ∼2%, the measured OA edge linewidth of InGaN epilayers matches that predicted by the random alloy model. A progressive deviation of the linewidth values expected from random alloying is then observed for InGaN epilayers with the increasing indium content for the remaining range spanning from ∼3 to nearly 18% of indium.

In order to gain additional insights into this deviation from the random alloy model, room temperature (RT) scanning near-field optical microscope (SNOM) mappings were carried out. These measurements offer a spatial resolution (∼100 nm) about one order of magnitude better than that accessible through OA measurements (spot size of ∼2 μm) while giving simultaneous access to the surface morphology through the feedback signal of the SNOM tuning fork. In Fig. 3(b), the RT near-field lowest emission linewidth (filled red dots) deduced from SNOM mappings is reported as a function of OA excitonic energy. In addition, the value of

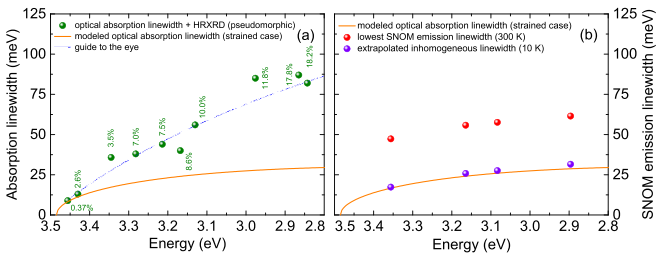

FIG. 3. (a) LT ($T = 10$ K) OA edge linewidth (filled green dots) as a function of OA excitonic energy of several $In_xGa_{1-x}N$ epilayers pseudomorphic to GaN whose indium content has been deduced from HRXRD measurements. The blue line is a guide to the eye for the evolution of the LT OA edge linewidth. (b) Lowest emission linewidth (filled red dots) as a function of OA excitonic energy deduced from RT SNOM mappings. The filled violet dots correspond to the extrapolated inhomogeneous linewidth. The calculated dependence of the linewidth for a random alloy is reported for the fully strained case (orange line) in the two subfigures.

the inhomogeneous linewidth (filled violet dots) was extrapolated by making use of the relationship linking the total linewidth Γ to the homogeneous (Γ_h) and the inhomogeneous (Γ_{inh}) linewidths given by $\Gamma = \Gamma_h + \Gamma_{inh}$,[33] assuming as a first approximation no energy blueshift with decreasing temperature of the optical transition. A reasonable RT homogeneous broadening value of 30 meV was considered for illustration purposes,[34] which leads to a good agreement between the modeled LT OA linewidth (orange line) and SNOM data. Therefore, it shows that for some specific locations, the high spatial resolution offered by SNOM (∼100 nm) allows probing regions where the alloy broadening is governed by random atomic disorder even for the largest indium contents investigated in this work (∼18%). Through the comparison of these values with the measured OA linewidths, one can infer that the meandering length scale is larger than the spatial resolution offered by SNOM imaging.

To be more quantitative in our analysis, the RT near-field mapping of the PL peak energy and that of the emission linewidth of an InGaN epilayer with an indium content of $2.6 \pm 0.1\%$ are shown in Figs. 4(a) and 4(b), respectively. The corresponding 10×10 μm^2 surface morphology map is displayed in Fig. 4(c). Beyond the small standard deviation ($\ll 1$ meV) of both the average peak energy and the average linewidth whose value is centered at ∼3.357 eV and 47.3 meV, respectively, we can notice the presence of elongated areas characterized by a slightly larger value for both quantities. Those areas appear to be closely linked to the surface morphology revealed by SNOM topography. In order to better illustrate this feature, similar maps are displayed in Figs. 4(d)–4(f) for an InGaN epilayer with an indium content of $11.8 \pm 0.9\%$ (HRXRD value), leading to a RT average peak energy of ∼2.960 eV and an average linewidth value of 60.5 meV. Note that the peak energy variation between 2.934 and 2.982 eV [Fig. 4(d)] corresponds to an indium content ranging between 12.2 and 13.6% based on Eq. (S3) of the supplementary material, assuming a 70 meV blueshift between RT and low temperature, with a mean of 12.9%, which is in good agreement with HRXRD data. As for the low indium content InGaN epilayer, we can notice regions that exhibit a larger linewidth than the average one by ∼4 meV with an excess reaching up to 10 meV. This anisotropic long-range disorder, extending over several microns, is ascribed to the underlying GaN template surface morphology. This picture is well supported by SNOM surface morphology maps recorded simultaneously to near-field PL ones that show long-range step-meandering features, whose signature becomes more apparent with increasing indium content [cf. Figs. 4(c) and 4(f)]. In fact, this morphology stems from the deposition of a few tens of nanometers of GaN at LT before the deposition of InGaN epilayers, which leads to surface roughening induced by the presence of an Ehrlich-Schwöbel barrier (ESB).[35] In addition, surface morphology images also reveal a much shorter range disorder inherent to the InGaN epilayers, which manifests itself by a spectral broadening in the SNOM spectra above the random alloy limit and is reminiscent of an ESB-induced surface roughening of the InGaN layer itself. Here, the related variations in the local step-edge density should likely affect the

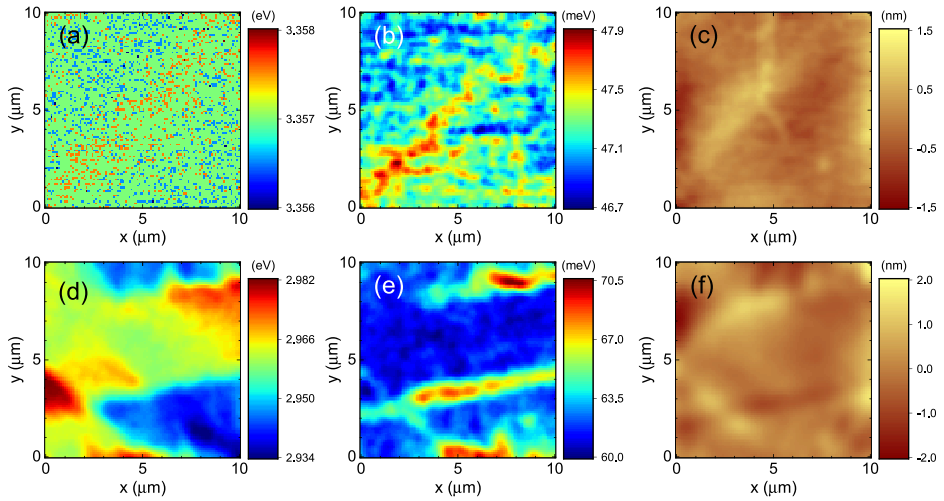

FIG. 4. (a) RT near-field mapping of the PL peak energy taken on a 100-nm-thick InGaN epilayer pseudomorphic to GaN with an indium content of 2.6% and (b) corresponding mapping of the RT PL emission linewidth. (c) $10 \times 10\ \mu m^2$ surface morphology map acquired simultaneously to the near-field PL mapping. (d) RT near-field mapping of the PL peak energy taken on a 25-nm-thick InGaN epilayer pseudomorphic to GaN with an indium content of 11.8% and (e) corresponding mapping of the RT PL emission linewidth. (f) $10 \times 10\ \mu m^2$ surface morphology map acquired simultaneously to the near-field PL mapping. The root mean square surface roughness values for the surface morphology maps (c) and (f) are equal to 0.35 and 0.48 nm, respectively.

incorporation of indium on a much shorter scale.[36] This picture is further supported by high-resolution atomic force microscopy (AFM) images and near-field PL mappings recorded on a 100-nm-thick InGaN epilayer with an indium content of $8.6 \pm 0.2\%$ [Figs. 5(a) and 5(b)]. Long-range step-meandering features are accompanied by a much shorter range disorder corresponding to meandering features related to the InGaN epilayer itself that is interspaced by a distance of ~500 nm ([cf. set of parallel dashed lines serving as guides to the eye in Fig. 5(b)].

To go one step further in our assessment of the optical properties of InGaN epilayers, it is tempting to draw a comparison between SNOM/AFM observations and the results reported in Fig. 3(a). The measured LT OA linewidth is shown to progressively deviate from the value expected for a random alloy. Such a feature can be ascribed to variations in the compositional disorder obviously occurring at a scale exceeding that probed by excitons, leading to a progressive breakdown of the pure random alloy picture. This heterogeneity stems from different local misorientations, and hence a position-dependent step-edge density, and the above-mentioned ESB that would be responsible for a change in the mean incorporation of indium atoms.[36] This twofold combination seems to be the main contribution to the inhomogeneous broadening of the OA edge for high indium contents. For instance, the random alloy model predicts an OA linewidth of 30 meV around 18% of indium, whereas we measured a value of 85 meV for our pseudomorphic InGaN epilayer. The remarkable point is that the InGaN alloy is certainly more sensitive to surface morphology than most of the usual ternary semiconducting alloys due to the very different growth conditions of III-nitride binaries[37] and the consequent need to reduce the growth temperature to allow for indium incorporation. Note that the latter aspect has also been shown to be especially dramatic in the case of the InAlN alloy.[38] Furthermore, strain fluctuations due to the large lattice-mismatch between InN and GaN will most likely affect more deeply the local indium incorporation with the increasing targeted indium content, hence further enhancing alloy disorder.

The present study shows that random alloy disorder is the main source of OA edge broadening in these pseudomorphic InGaN epilayers only for very low indium contents ($x < 2\%$). An increase in the OA edge linewidth is observed with increasing indium content that is due to preexisting surface roughness and growth front roughening originating from ESB phenomena. This ESB-induced surface morphology roughening is likely less prominent, or even absent, in thin InGaN layers such as QWs. Therefore, for well-controlled QW thicknesses, inhomogeneous broadening purely due to random alloy disorder can be achieved in InGaN/GaN QWs even for high indium contents.[39] Note in this respect that the reported inhomogeneous linewidth broadening values of InGaN QWs extracted from gain spectra in state of the art cyan-green wavelength III-nitride LDs indeed exhibit a moderate increase over this wavelength range.[40,41] Finally, let us emphasize that the ability to control the surface morphology and hence the homogeneity of thick InGaN epilayers is extremely relevant in the framework of applications where the minimization of unwanted disorder is critical. This is especially the case when attempts are made to realize laser waveguides,[42] metamorphic layers,[43] or solar cells.[44,45]

To conclude, the structural and optical properties of pseudomorphic $In_xGa_{1-x}N$ ($0 < x < 0.18$) epilayers grown on low dislocation density *c*-plane FS GaN substrates have been characterized. Optical measurements giving access to the evolution of the LT OA edge linewidth clearly indicate that low indium content layers ($x < 2\%$) exhibit features that are accounted for by the random alloy model. However, for higher indium contents, the LT OA edge linewidth increases significantly. Complementary RT SNOM data providing simultaneous access to near-field PL and surface morphology clearly show a spatial correlation between step-meandering features and fluctuations observed in the emission properties of those epilayers. Interestingly, thanks to the high spatial

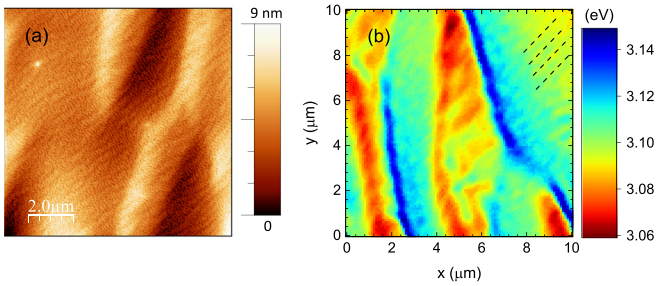

FIG. 5. (a) $10 \times 10\ \mu m^2$ high-resolution AFM scan showing short-range and long-range step-meandering features taken on a 100-nm-thick InGaN epilayer with an indium content of 8.6% and (b) RT near-field mapping, measured at a different location, of the PL peak energy taken on the same epilayer with the SNOM apparatus. The set of dashed lines serves as a guide to the eye to highlight short-range meanders stemming from the InGaN epilayer itself.

resolution offered by SNOM, the alloy broadening governed by random alloy atomic disorder could be probed at some specific locations even for the largest indium contents investigated in this work (∼18%). This study demonstrates that long-range fluctuations due to the surface morphology are the main source of OA edge broadening in thick InGaN epilayers.

See supplementary material for a description of (A) the experimental details, (B) the XRD RSM of a 100-nm-thick InGaN epilayer showing a signature of plastic relaxation, and the determination of (C) the absorption linewidth of a random wurtzite-based ternary alloy and (D) that of the transition energy of fully strained InGaN epilayers. Complementary optical features of InGaN epilayers are given in Sec. (E).

This work was supported by the Swiss National Science Foundation through Grant Nos. 200020-113542 and 200020-153620. The research at KTH was performed within the frame of Linnaeus Excellence Center for Advanced Optics and Photonics (ADOPT) and was financially supported by the Swedish Research Council (Contract No. 621-2013-4096).

[1]S. Nakamura, T. Mukai, and M. Senoh, Appl. Phys. Lett. **64**, 1687 (1994).
[2]Y. Narukawa, M. Ichikawa, D. Sanga, M. Sano, and T. Mukai, J. Phys. D: Appl. Phys. **43**, 354002 (2010).
[3]S. Nakamura, M. Senoh, S. Nagahama, N. Iwasa, T. Yamada, T. Matsushita, H. Kiyoku, and Y. Sugimoto, Jpn. J. Appl. Phys., Part 2 **35**, L74 (1996).
[4]S. Nakamura, Science **281**, 956 (1998).
[5]I. Ho and G. B. Stringfellow, Appl. Phys. Lett. **69**, 2701 (1996).
[6]S. Chichibu, T. Azuhata, T. Sota, and S. Nakamura, Appl. Phys. Lett. **69**, 4188 (1996).
[7]Y. Narukawa, Y. Kawakami, S. Fujita, S. Fujita, and S. Nakamura, Phys. Rev. B **55**, R1938 (1997).
[8]T. M. Smeeton, M. J. Kappers, J. S. Barnard, M. E. Vickers, and C. J. Humphreys, Appl. Phys. Lett. **83**, 5419 (2003).
[9]P. R. C. Kent and A. Zunger, Appl. Phys. Lett. **79**, 1977 (2001).
[10]L.-W. Wang, Phys. Rev. B **63**, 245107 (2001).
[11]S. F. Chichibu, A. Uedono, T. Onuma, B. A. Haskell, A. Chakraborty, T. Koyama, P. T. Fini, S. Keller, S. P. DenBaars, J. S. Speck, U. K. Mishra, S. Nakamura, S. Yamaguchi, S. Kamiyama, H. Amano, I. Akasaki, J. Han, and T. Sota, Nat. Mater. **5**, 810 (2006).
[12]M. Filoche, M. Piccardo, Y.-R. Wu, C.-K. Li, C. Weisbuch, and S. Mayboroda, Phys. Rev. B **95**, 144204 (2017).
[13]M. Piccardo, C.-K. Li, Y.-R. Wu, J. S. Speck, B. Bonef, R. M. Farrell, M. Filoche, L. Martinelli, J. Peretti, and C. Weisbuch, Phys. Rev. B **95**, 144205 (2017).
[14]C.-K. Li, M. Piccardo, L.-S. Lu, S. Mayboroda, L. Martinelli, J. Peretti, J. S. Speck, C. Weisbuch, M. Filoche, and Y.-R. Wu, Phys. Rev. B **95**, 144206 (2017).
[15]F. Natali, D. Byrne, M. Leroux, B. Damilano, F. Semond, A. Le Louarn, S. Vezian, N. Grandjean, and J. Massies, Phys. Rev. B **71**, 075311 (2005).
[16]M. Shahmohammadi, W. Liu, G. Rossbach, L. Lahourcade, A. Dussaigne, C. Bougerol, R. Butté, N. Grandjean, B. Deveaud, and G. Jacopin, Phys. Rev. B **95**, 125314 (2017).
[17]C. Wetzel, T. Takeuchi, S. Yamaguchi, H. Katoh, H. Amano, and I. Akasaki, Appl. Phys. Lett. **73**, 1994 (1998).
[18]W. Shan, W. Walukiewicz, E. E. Haller, B. D. Little, J. J. Song, M. D. McCluskey, N. M. Johnson, Z. C. Feng, M. Schurman, and R. A. Stall, J. Appl. Phys. **84**, 4452 (1998).
[19]R. W. Martin, P. G. Middleton, K. P. O'Donnell, and W. Van der Stricht, Appl. Phys. Lett. **74**, 263 (1999).
[20]C. Wetzel, T. Takeuchi, H. Amano, and I. Akasaki, J. Appl. Phys. **85**, 3786 (1999).
[21]H. P. D. Schenk, M. Leroux, and P. de Mierry, J. Appl. Phys. **88**, 1525 (2000).
[22]S. Srinivasan, F. Bertram, A. Bell, F. A. Ponce, S. Tanaka, H. Omiya, and Y. Nakagawa, Appl. Phys. Lett. **80**, 550 (2002).
[23]C. Sasaki, H. Naito, M. Iwata, H. Kudo, Y. Yamada, T. Taguchi, T. Jyouichi, H. Okagawa, K. Tadatomo, and H. Tanaka, J. Appl. Phys. **93**, 1642 (2003).
[24]M. D. McCluskey, C. G. Van de Walle, L. T. Romano, B. S. Krusor, and N. M. Johnson, J. Appl. Phys. **93**, 4340 (2003).
[25]A. Rosenauer, T. Mehrtens, K. Müller, K. Gries, M. Schowalter, P. Venkata Satyam, S. Bley, C. Tessarek, D. Hommel, K. Sebald, M. Seyfried, J. Gutowski, A. Avramescu, K. Engl, and S. Lutgen, Ultramicroscopy **111**, 1316 (2011).
[26]T. Schulz, T. Remmele, T. Markurt, M. Korytov, and M. Albrecht, J. Appl. Phys. **112**, 033106 (2012).
[27]M. Vladimirova, A. Pimpinelli, and A. Videcoq, J. Cryst. Growth **220**, 631 (2000).
[28]E. F. Schubert, E. O. Göbel, Y. Horikoshi, K. Ploog, and H. J. Queisser, Phys. Rev. B **30**, 813 (1984).
[29]E. Feltin, A. Castiglia, G. Cosendey, L. Sulmoni, J.-F. Carlin, N. Grandjean, M. Rossetti, J. Dorsaz, V. Laino, M. Duelk, and C. Velez, Appl. Phys. Lett. **95**, 081107 (2009).
[30]M. Pristovsek, Appl. Phys. Lett. **102**, 242105 (2013).
[31]S. Pereira, M. R. Correia, E. Pereira, K. P. O'Donnell, C. Trager-Cowan, F. Sweeney, and E. Alves, Phys. Rev. B **64**, 205311 (2001).
[32]P. Sohi, D. Martin, and N. Grandjean, Semicond. Sci. Technol. **32**, 075010 (2017).
[33]S. Rudin, T. L. Reinecke, and B. Segall, Phys. Rev. B **42**, 11218 (1990).
[34]R. Butté, G. Christmann, E. Feltin, J.-F. Carlin, M. Mosca, M. Ilegems, and N. Grandjean, Phys. Rev. B **73**, 033315 (2006).
[35]N. A. K. Kaufmann, L. Lahourcade, B. Hourahine, D. Martin, and N. Grandjean, J. Cryst. Growth **433**, 36 (2016).
[36]M. Leszczynski, R. Czernecki, S. Krukowski, M. Krysko, G. Targowski, P. Prystawko, J. Plesiewicz, P. Perlin, and T. Suski, J. Cryst. Growth **318**, 496 (2011).
[37]H. Morkoç, *Handbook of Nitride Semiconductors and Devices, Materials Properties, Physics and Growth* (Wiley-VCH, Weinheim, 2008), Vol. 1.
[38]G. Perillat-Merceroz, G. Cosendey, J.-F. Carlin, R. Butté, and N. Grandjean, J. Appl. Phys. **113**, 063506 (2013).
[39]A. David and M. J. Grundmann, Appl. Phys. Lett. **97**, 033501 (2010).
[40]T. Lermer, A. Gomez-Iglesias, M. Sabathil, J. Müller, S. Lutgen, U. Strauss, B. Pasenow, J. Hader, J. V. Moloney, S. W. Koch, W. Scheibenzuber, and U. T. Schwarz, Appl. Phys. Lett. **98**, 021115 (2011).
[41]M. Funato, Y. S. Kim, Y. Ochi, A. Kaneta, Y. Kawakami, T. Miyoshi, and S. Nagahama, Appl. Phys. Express **6**, 122704 (2013).
[42]T. Lermer, M. Schillgalies, A. Breidenassel, D. Queren, C. Eichler, A. Avramescu, J. Müller, W. Scheibenzuber, U. Schwarz, S. Lutgen, and U. Strauss, Phys. Status Solidi A **207**, 1328 (2010).
[43]K. Hestroffer, F. Wu, H. Li, C. Lund, S. Keller, J. S. Speck, and U. K. Mishra, Semicond. Sci. Technol. **30**, 105015 (2015).
[44]J. Wu, W. Walukiewicz, K. M. Yu, W. Shan, J. W. Ager III, E. E. Haller, H. Lu, W. J. Schaff, W. K. Metzger, and S. Kurtz, J. Appl. Phys. **94**, 6477 (2003).
[45]A. G. Bhuiyan, K. Sugita, A. Hashimoto, and A. Yamamoto, IEEE J. Photovolt. **2**, 276 (2012).